

# Specific heat study of the magnetocaloric effect in the Haldane-gap $S = 1$ spin-chain material $[\text{Ni}(\text{C}_2\text{H}_8\text{N}_2)_2\text{NO}_2](\text{BF}_4)$

M. Orendáč,<sup>1</sup> R. Tarasenko,<sup>1,2</sup> V. Tkáč,<sup>1,2</sup> A. Orendáčová,<sup>1</sup> and V. Sechovský<sup>2</sup>

<sup>1</sup>*Institute of Physics, P. J. Šafárik University, Park Angelinum 9, 041 54 Košice, Slovak Republic*

<sup>2</sup>*Faculty of Mathematics and Physics, Department of Condensed Matter Physics, Charles University, Ke Karlovu 5, 121 16 Prague 2, Czech Republic*

(Received 17 May 2017; revised manuscript received 17 July 2017; published 20 September 2017)

Magnetocaloric effect in the Haldane-gap  $S = 1$  spin-chain  $[\text{Ni}(\text{C}_2\text{H}_8\text{N}_2)_2\text{NO}_2](\text{BF}_4)$  was investigated at low temperatures ( $k_B T \ll J$ ) and magnetic fields up to nominally  $0.1 B_{\text{sat}}$ , where  $J$  and  $B_{\text{sat}}$  denote an exchange interaction and saturation magnetic field, respectively. Magnetic entropy was found to scale as  $\exp(\Delta/k_B T)$  in zero magnetic field and  $T^{0.67}$  for  $B = B_c$ , in which the Haldane gap should be closed, in reasonable agreement with the theoretical predictions. The existence of the inverse magnetocaloric effect for  $B < B_c$  was confirmed. The occurrence of normal magnetocaloric response at lowest temperatures and magnetic fields was attributed to  $S = 1/2$  degrees of freedom arising from the ends of chain segments.

DOI: [10.1103/PhysRevB.96.094425](https://doi.org/10.1103/PhysRevB.96.094425)

## I. INTRODUCTION

Magnetocaloric effect (MCE) describing the temperature change of a substance if exposed to the adiabatic change of a magnetic field has become a standard cooling technique for reaching low temperatures for decades [1]. The fact that the cooling rate  $(dT/dH)_S$  is given by a change of the magnetization with temperature  $(dM/dT)_H$ , stimulated interest in new phenomena accompanied by a pronounced change of the latter quantity. Consequently, apart from traditionally used systems involving electronic and/or nuclear degrees of freedom in paramagnetic salts [2–4], and materials magnetically ordering near room temperature [5], new unconventional materials have been explored. For example, enhanced MCE was theoretically predicted [6] and subsequently observed [7] in geometrically frustrated systems in the vicinity of the saturation field.

Recently, MCE attracted renewed attention in low-dimensional quantum spin systems, predominantly quantum spin chains. In these materials, there exist a quantum phase transition (QPT) induced by magnetic field separating an ordered state from a quantum disordered state. Moving the system through QPT is accompanied by a pronounced change of magnetic entropy and consequently large MCE may be anticipated. The isentropes of a uniformed  $S = 1/2$  Heisenberg chain have been studied numerically [8], the quantum transfer matrix technique adopted for  $S = 1/2$  XXZ chain confirmed an enhanced MCE in the vicinity of QPT. In addition, linear scaling of the magnetic entropy with temperature  $T$  in the gapless Luttinger-liquid state and scaling as  $\sqrt{T}$  at the field-induced transition to a gapped phase were predicted [9]. More complicated  $S = 1/2$  magnetic chains, namely  $J_1 - J_2$  and sawtooth chain [10], diamond chain [11],  $S = 1/2$  XX chain with three-spin interactions [12], were theoretically investigated and enhanced MCE at QPT was found. Notably, similar behavior was predicted also for a two-dimensional, frustrated square lattice  $J_1 - J_2$  system [13]. However, MCE study in two-dimensional (2D) coupled spin-dimer systems suggested that anomalies in cooling rate are not directly associated with a quantum phase transition or the

finite-temperature Berezinsky-Kosterlitz-Thouless transition [14].

Experimentally, MCE studies in  $S = 1/2$  Heisenberg chains confirmed the predicted behavior. More specifically, the investigation of cooling rate in  $[\text{Cu}(m\text{-C}_2\text{O}_4)(4\text{-aminopyridine})_2(\text{H}_2\text{O})]_n$  representing very good realization of an  $S = 1/2$  uniform Heisenberg antiferromagnetic chain [15] characterized by quantum critical behavior given by Luttinger liquid revealed an enhancement of MCE close to QCP [16]. Similar results were found in our previous studies of field-induced magnetic entropy change in another  $S = 1/2$  Heisenberg antiferromagnetic chain, namely  $\text{Cu}(dmbpy)(\text{H}_2\text{O})_2\text{SO}_4$  [17]. The investigation of the phase diagram of  $\text{Cu}(\text{NO}_3)_2 \cdot 2.5\text{D}_2\text{O}$  representing a quasi-one-dimensional (1D)  $S = 1/2$  alternating Heisenberg antiferromagnetic chain confirmed the predicted Luttinger liquid regime and a three-dimensional (3D) long-range ordered phase for various magnetic fields and temperatures [18].

In contrast, much less attention has been devoted to quantum spin chains with higher spins. Theoretical investigation of an ( $S = 5/2$ ,  $S = 1$ ) ferrimagnetic chain suggested enhanced MCE at the boundary of a ground state magnetization plateau and field-induced QCP at the critical magnetic field destroying the plateau was proposed [19]. Numerical studies involving an exact diagonalization and quantum Monte Carlo simulations of MCE in uniform  $S = 1$  Heisenberg antiferromagnetic chains suggested a possibility of cooling by closing the Haldane-gap  $\Delta$  by the magnetic field. In addition, scaling the entropy as  $\exp(\Delta/k_B T)$  in zero magnetic field and  $\sqrt{T}$  at a field-induced transition to a gapless phase, were proposed [8]. With respect to an experiment, we are unaware of any experimental studies of  $S = 1$  antiferromagnetic chain focused on its magnetothermal response.

The current work addresses magnetocaloric properties of a quantum spin chain with the Haldane gap,  $[\text{Ni}(\text{C}_2\text{H}_8\text{N}_2)_2\text{NO}_2](\text{BF}_4)$  (NENB). Previous investigation of NENB involving high field electron-spin resonance and a susceptibility study confirmed the existence of the Haldane phase in NENB and enabled the estimation of the Haldane gap

$\Delta/k_B = 17.4$  K, planar anisotropy  $D/k_B = 7.5$  K, rhombic anisotropy  $E/k_B = 0.7$  K, and  $g = 2.14$  [20]. In addition, the magnetic torque measurements reported in Ref. [20] confirmed the anisotropy in magnetic fields closing the Haldane gap, which was proposed by high field magnetization studies [21]. To the best of our knowledge, specific heat as well as direct magnetocaloric measurements of NENB have not been performed yet.

Our systematic study of specific heat of NENB has been performed at low temperatures and magnetic fields up to  $B \approx 0.1 B_{\text{sat}}$ . The specific heat data enabled the construction of the diagram of the temperature dependence of the entropy for various magnetic fields. The obtained isentropes confirmed the predicted inverse magnetocaloric effect in the Haldane phase and revealed a pronounced change of the regime when closing the Haldane gap. The analyses of the temperature dependences of the entropy support the proposed scaling in both zero magnetic field and the magnetic field closing the Haldane gap. The observed deviations from the theoretical predictions are attributed to the differences between intrinsic properties of NENB and an ideal model behavior.

## II. CRYSTAL STRUCTURE AND EXPERIMENTAL DETAILS

Single crystals of NENB of nominally 4 mm length and  $2 \text{ mm}^2$  cross section were grown by a well established procedure based on the reaction of  $[\text{Ni}(\text{C}_2\text{H}_8\text{N}_2)_3](\text{BF}_4)_2$  with  $\text{Ni}(\text{BF}_4)_2 \cdot 6\text{H}_2\text{O}$  and  $\text{NaNO}_2$  in aqueous solution. Subsequent x-ray analysis confirmed the existence of a single phase. The compound crystallizes in an orthorhombic structure, space group  $Pnma$  with dimensions of unit cell  $a = 15.0373(5)$  Å,  $b = 10.2276(3)$  Å, and  $c = 7.9719(2)$  Å,  $Z = 4$  [22]. The structure of NENB consists of  $S = 1$  chains running along the  $b$  axis of the crystal. Within the chains, Ni(II) ions are pseudo-octahedrally coordinated. Four N atoms from two ethylenediamine ( $\text{C}_2\text{H}_8\text{N}_2$ ) units are located in the equatorial plane of the octahedron in a slightly distorted square planar coordination.

Two adjacent equatorial planes are canted in angle  $14.1^\circ$ . The exchange bridge between neighboring Ni(II) ions is created by N and O atoms from the  $[\text{NO}_2]^-$  unit. The chains are well separated by  $[\text{BF}_4]^-$  anions. The structure contains a single Ni(II) site, however disorder exists in the location of  $[\text{NO}_2]^-$  units. The structural considerations suggest that the  $\text{NO}_2^-$  units are ordered along each chain and the orientations of chains are randomly distributed [23].

Specific heat measurements of 1.4 mg single crystal were performed using the Quantum Design PPMS system with  $^3\text{He}$  insert. The external magnetic field was oriented along the  $b$  axis of the crystal. The contribution of the addenda was subtracted from the total specific heat data.

## III. RESULTS

Systematic studies of specific heat were performed at temperature range 0.4–25 K in magnetic fields up to 14 T. For temperatures lower than nominally 5 K two regimes can be distinguished, see Fig. 1. The effect of lower magnetic fields, in our case below 9 T, is manifested only by increasing specific

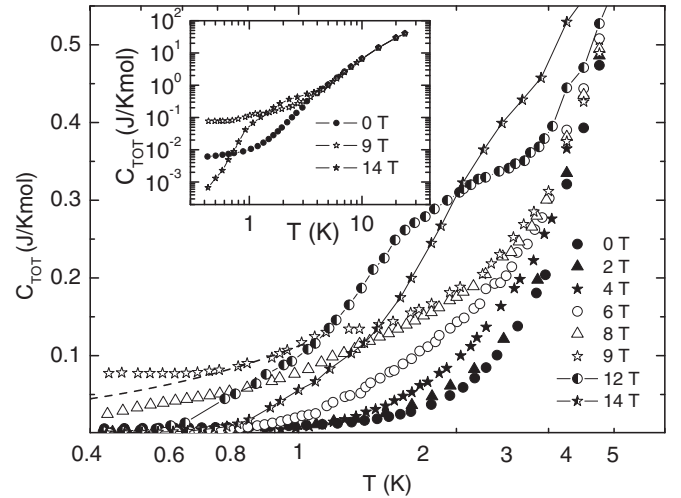


FIG. 1. Temperature dependence of specific heat of NENB studied at various magnetic fields oriented along the  $b$  axis of the crystal below 5 K. The dashed line denotes the extrapolation of the specific heat data at 9 T. See text for a more detailed discussion. Inset: Selected specific heat data of NENB from 0.4 to 25 K.

heat for temperatures lower than nominally 3 K. Such a behavior indicates the onset of an inverse magnetocaloric effect. On the other hand, magnetic fields higher than 9 T suppress specific heat forming a small bump, which is shifted towards higher temperatures with increasing magnetic fields. All specific heat data tend to merge at temperatures higher than 5 K.

Since NENB represents a magnetic insulator only magnetic and lattice components of specific heat contribute to the total signal. A larger value of the exchange interaction in NENB ( $J/k_B \approx -42$  K) prevents us from adopting a simple low-temperature Debye approximation since magnetic contribution to the specific heat extends to higher temperatures, where the low-temperature approximation may not be valid anymore. Consequently, the specific heat was expressed as

$$C_{\text{tot}}(T) = C_{\text{mag}}(T) + 9rR \left( \frac{T}{\theta_D} \right)^3 \int_0^{\frac{\theta_D}{T}} \frac{x^4 e^x}{(e^x - 1)^2} dx \quad (1)$$

in which the first term represents a magnetic contribution and the second one the lattice specific heat calculated using a Debye model. The magnetic contribution can be evaluated adopting numerical results [24], for NENB the data are available from 9 K. Notably, the prediction for an isotropic  $S = 1$  Heisenberg antiferromagnetic chain (1D HAF) was used despite the fact that in NENB single-ion anisotropy expressed by  $D/k_B = 7.5$  K and  $|E/k_B| = 0.5$  K was found [20]. Such an approach is adequate for NENB with  $D/J = 0.2$  since the available numerical predictions for specific heats of 1D HAF with  $D/J = 0$  and  $D/J = 2$  differ by only a few percent in a wide temperature range involving also the round maximum [24].

In the second term,  $r$  represents the number of independent vibrating groups,  $\theta_D$  denotes Debye temperature, and  $R$  stands for a universal gas constant. Considering the structure of NENB, the value  $r = 5$  was adopted for specific heat analysis. In order to determine the value of  $\theta_D$ , specific heat of isotropic 1D HAF with  $J/k_B = -42$  K was subtracted from the exper-

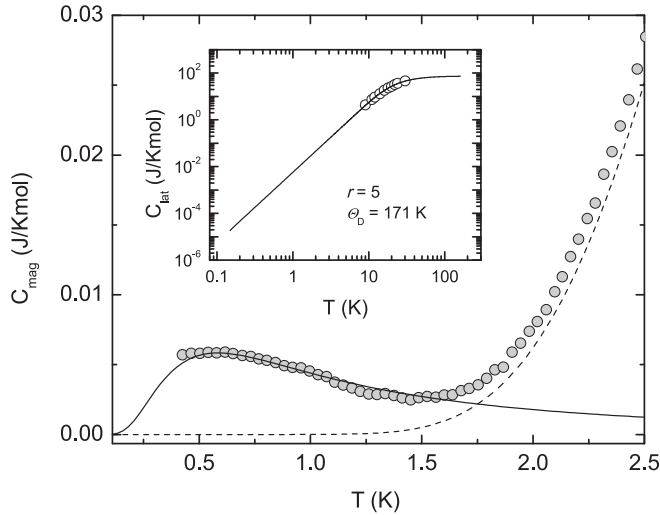


FIG. 2. Low-temperature part of the magnetic specific heat of NENB in zero magnetic field (full circles) analyzed using Eq. (2) (dashed line). The contribution of ferromagnetic dimers with  $J_d/k_B = 0.6$  K and  $x_d = 0.003$ , respectively, is represented by a solid line. Inset: The analysis of the lattice contribution (open circles) using Eq. (1) (solid line). For clarity, only selected points are plotted.

imental data obtained from 9 to 25 K. The resulting specific heat was attributed to the lattice contribution and was analyzed using a Debye model. The analysis yielded  $\theta_D = 171$  K and confirmed that below 10 K, low-temperature approximation for lattice specific heat is adequate, see inset in Fig. 2. Notably, the obtained value of the Debye temperature is comparable with  $\theta_D = 132$  K proposed for another Haldane-gap system  $(\text{CH}_3)_4\text{NNi}(\text{NO}_2)_3$ , commonly abbreviated as TMNIN [25]. Consequently, below 9 K, low-temperature approximation was used to obtain a magnetic specific heat of NENB from the experimental data.

#### IV. DISCUSSION

Closer inspection of a magnetic specific heat of NENB for temperatures lower than 3 K in zero magnetic field reveals two characteristic features: rapid drop of specific heat with decreasing temperature down to 1.5 K and the formation of a small round maximum at about 0.6 K, see Fig. 2. Exponential-like decay of specific heat may be associated with depopulation of the excited states at temperatures  $k_B T \ll \Delta$ . Following the approach from Ref. [25] in the first approximation only the ground state and the first excited state are considered and magnetic specific heat is expressed as

$$C_{\text{mag}}(T) = \gamma N_A k \left( \frac{\Delta}{k_B T} \right)^2 \left( \frac{g_1}{g_2} \right) \exp \left( - \frac{\Delta}{k_B T} \right) \quad (2)$$

where  $\gamma$  is a reduction factor,  $N_A$  denotes Avogadro's number, and  $g_0$  and  $g_1$  are degeneracies of the ground and the first excited states, respectively. Fixing the value of the gap  $\Delta = 0.41$  J,  $\gamma(g_1/g_0)$  remains the only free parameter. The exponential decay of specific heat data can be reasonably described with  $\gamma(g_1/g_0) = 0.090$ , which agrees remarkably well with  $\gamma(g_1/g_0) = 0.092$  found for the canonical Haldane-

gap system NENP. In contrast,  $\gamma(g_1/g_0) = 0.19$  reported for TMNIN is nearly two times higher [25].

The broad maximum located at 0.6 K in zero magnetic field suggests the presence of other degrees of freedom. Obviously it cannot be ascribed to paramagnetic impurities, instead  $S = 1/2$  states from the ends of chain segments can be considered. These states were predicted by a valence bond solid model [26] and experimentally found in NENP and other Haldane-gap chains [27]. The magnetic interactions between the end states within one chain segment are expected to be negligible for long enough segments ( $> 2\xi$ ),  $\xi$  denotes magnetic correlation length. Nevertheless, exchange coupling between the end states from various segments may still exist. Such a possibility was explored in Ref. [28], more specifically, it was proposed that in  $\text{NiC}_2\text{O}_4 \cdot 2[2\text{Miz}]_x \cdot \text{H}_2\text{O}_{1-x}$  the end chain defects are created by a displacement of the intervening anions  $[\text{ClO}_4]^{2-}$  at the end of segments towards an adjacent segment. This displacement gives rise to ferromagnetic coupling between the end spins. The coexistence of the ferromagnetic coupling, intra and interchain coupling leads to the onset of a spin glass state, which in  $\text{NiC}_2\text{O}_4 \cdot 2[2\text{Miz}]_x \cdot \text{H}_2\text{O}_{1-x}$  was confirmed for  $x > 0.078$  [28]. It should be noted that susceptibility studies of NENB performed in various magnetic fields indicated behavior consistent with the spin glass state, however, this state is suppressed for magnetic fields higher than 0.1 T [20]. Consequently, in the first approximation, the broad maximum in specific heat of NENB was ascribed to  $S = 1/2$  ferromagnetic dimers with a single magnitude of the exchange interaction, the corresponding fit yielded  $J_d/k_B = 0.6$  K and  $x_d = 0.003$ , where  $J_d$  and  $x_d$  denote intradimer interaction and concentration of the dimers, respectively. Notably, the used approximation led to very good agreement with the experimental data and reasonable values of both parameters.

Determination of magnetic specific heat of 1D HAF itself enables the examination of scaling of the magnetic entropy with temperature. Unlike the  $S = 1/2$  antiferromagnetic chain, in which Luttinger spin liquid state leads to  $T$  scaling in zero magnetic field, quantum Monte Carlo calculations performed for  $S = 1$  1D HAF suggested that the entropy should asymptotically behave as  $S(T) = A^{\text{theor}} \exp(-\Delta/k_B T)$  [8]. The asymptotical behavior was predicted for temperatures below nominally  $0.35$  J/ $k_B$  and  $A^{\text{theor}} = 4.79$  J/(K mol) was proposed. The experimental data were analyzed using the proposed behavior of the entropy after the subtraction of the contribution of end chain spins and with fixed  $\Delta = 0.41$  J, see Fig. 3. Very good agreement is found up to 12 K ( $0.29$  J/ $k_B$ ), for higher temperatures the entropy tends to deviate towards higher values in accord with the numerical calculations. A small deviation persisting at low temperatures can be attributed to the approximation used for the analysis of the broad anomaly. On the other hand,  $A^{\text{expt}} = 2.5$  J/(K mol) obtained from the analysis is nearly two times smaller than that proposed by the calculation. The origin of this discrepancy has not been clarified yet. One might speculate that the difference between  $A^{\text{theor}}$  and  $A^{\text{expt}}$  is potentially related to different  $\gamma(g_1/g_0)$  values found for various Haldane-gap systems. Consequently, for TMNIN, good agreement between  $A^{\text{theor}}$  and  $A^{\text{expt}}$  might be anticipated. Potentially, single-ion anisotropy might play a role, since  $D/J = 0.2$  was found for NENP and NENB, whereas TMNIN is characterized by  $D \approx 0$ . In

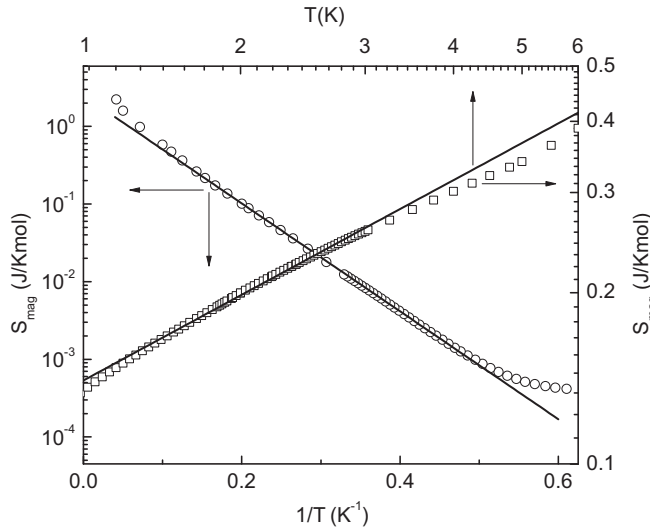


FIG. 3. Temperature dependence of magnetic entropy of NENB in magnetic fields  $B = 0$  (open circles), and  $B = B_c \approx 9$  T (open squares) in the corresponding coordinates. Solid lines represent fits using the predictions  $S(T) \approx \exp(\Delta/k_B T)$  and  $S(T) \approx T^\beta$  for  $B = 9$  T, respectively.

this context, systematic studies of the entropy behavior at  $T \ll \Delta/k_B$  for  $S = 1$  1D HAF with different  $D/J$  ratio would be informative.

Closing the Haldane gap by magnetic field drives the system to the vicinity of a quantum phase transition. In this region a large number of low-lying states are present and magnetic correlation length grows rapidly,  $\xi \rightarrow \infty$ . In one-dimensional systems the entropy was predicted to scale as  $\sqrt{T}$  at quantum phase transition [29]. The predicted dependence was supported by numerical study of the asymptotical behavior of the entropy for isotropic  $S = 1$  1D HAF, where  $\sqrt{T}$  dependence was found for  $0.03 < T/J < 0.09$  [8]. Magnetic torque measurements of NENB were performed in order to determine  $B_c^{\text{par}} = 9$  T and  $B_c^{\text{perp}} = 10$  T, the critical fields oriented parallel and perpendicular to the chains, respectively [20].

Consequently, after subtracting the contributions of phonons and  $S = 1/2$  ferromagnetic dimers the temperature dependence of magnetic entropy was calculated from the specific heat studied at 9 T and the results are presented in Fig. 3. Following the theoretical prediction the entropy was fitted using the relation  $S(T) = b^{\text{expt}} T^\beta$  and the analysis yielded  $b^{\text{expt}} = 0.67 \text{ J}/(\text{K}^{\beta-1} \text{ mol})$  and  $\beta = 0.67$ . Satisfactory agreement is found in the temperature range from  $0.03T/J$  (1.3 K) to  $0.09T/J$  (3.1 K), and the found exponent  $\beta$  corresponds reasonably with the theoretically proposed value 0.5. The remaining difference may be attributed to the structural features of NENB. More specifically, since the adjacent equatorial planes of successive Ni(II) units are canted by an angle of  $14.1^\circ$ , the orientation of magnetic field exactly parallel to all local anisotropy axes is not possible. The sensitivity of the orientation of magnetic field to local anisotropy axis was demonstrated in magnetization studies of NENB [21], where for perpendicular magnetic fields lower than  $B_c^{\text{par}}$ , much higher magnetization was observed than for parallel orientation. Consequently, a small misalignment between a local anisotropy axis and the direction of magnetic field may

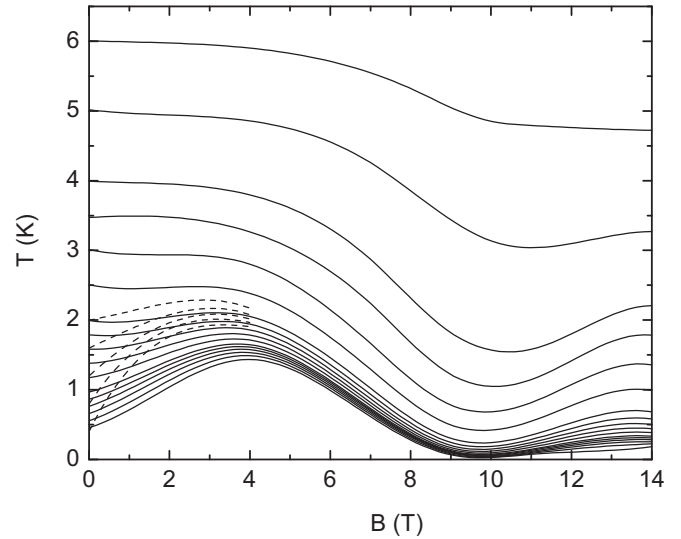


FIG. 4. Adiabatic demagnetization curves for NENB calculated from magnetic entropy (solid lines). The contribution of ferromagnetic dimers with  $J_d/k_B = 0.6$  K and  $x_d = 0.003$ , respectively, is represented by dashed lines.

have a pronounced influence on thermodynamic quantities in NENB. With respect to the magnitude of parameter  $b^{\text{expt}}$ , a similar situation as for zero magnetic field is found, namely, theoretically proposed  $b^{\text{theor}} = 1.10 \text{ J}/(\text{K}^{1.5} \text{ mol})$  is nearly twice higher than  $b^{\text{expt}}$ .

Systematic study of specific heat in magnetic fields up to 14 T enabled the calculation of the magnetic entropy as a function of the temperature for various magnetic fields and subsequently the construction of the isentropes, i.e., adiabatic demagnetization curves, these are illustrated in Fig. 4. It should be noted that simple exponential extrapolation of the specific heat from the lowest measured temperature to zero was used for the calculation of the entropy and subsequently for the isentropes. This simplified approach was found to be adequate for the forthcoming discussion, since other extrapolations (e.g., power) performed for selected magnetic fields did not substantially alter the properties of isentropes. Specific heat data studied at 9 T represent the only exception, where the extrapolation was made without considering a small increase of specific heat with decreasing temperature, see Fig. 1. Using the aforementioned extrapolation weakens the calculated inverse magnetocaloric effect in the vicinity of 9 T, nevertheless, the other properties of isentropes should not be influenced significantly. The observed increase can be attributed to field-induced magnetic order occurring below 0.4 K. The effect of the field-induced long-range ordering is discussed in more detail below.

In Fig. 4 two regimes can be clearly distinguished. Inverse magnetocaloric effect, which is becoming more pronounced with decreasing temperature, exists for  $T > 2$  K and magnetic fields lower than  $B_c$ . In contrast, for magnetic fields higher than  $B_c$  and low temperatures weak normal magnetocaloric effect occurs which tends to diminish with increasing temperature. Thus for a chain with the Haldane gap and  $T \ll J/k_B$ ,  $B > B_c$  an uncommon situation is observed where a magnetic system containing interacting spins nearly does not thermally respond

on adiabatic (de)magnetization. Notably, similar behavior may be anticipated in systems with magnetization plateaus and for uniform  $S = 1/2$  antiferromagnetic chains in low magnetic fields and  $T \approx 0.8 J/k_B$  [9]. The aforementioned features coincide very well with the theoretical predictions supporting theoretically proposed magnetocaloric behavior of a quantum spin chain with the Haldane gap for magnetic fields lower than  $B_{\text{sat}}$  [8]. However, for  $T < 2$  K and  $B < 4$  T normal magnetocaloric effect was found to dominate the predicted inverse one. Various reasons can be considered to clarify the difference. First of all, one should think of the aforementioned misalignment between the local anisotropy axis and the direction of the magnetic field. Despite the proved sensitivity of thermodynamic quantities of NENB with respect to the orientation of the magnetic field, magnetizations for both parallel and perpendicular magnetic fields rise monotonically with increasing magnetic field up to 9 T [21] giving no reason for the sign change in  $(dT/dB)_S$  dependence observed for  $T < 2$  K and in  $B \approx 4$  T.

The isentropes might be influenced by the interchain exchange coupling, which is present in all real quantum spin chains. The Haldane gap is known to be robust against small interchain interaction  $J'$  ( $z'J' \ll J$ ,  $z'$  denotes the number of adjacent chains) [30]. Nevertheless, the combination of magnetic field and small enough interchain coupling is known to lead to magnetic field-induced long-range ordering at magnetic fields smaller than  $B_c$ . The ordering can be described as the three-dimensional Bose-Einstein condensation of the lower-branch triplets and obviously should be manifested as a  $\lambda$ -like anomaly in specific heat [31]. The field-induced long-range ordering was experimentally studied in spin-1 chain compound  $\text{Ni}(\text{C}_5\text{H}_{14}\text{N}_2)_2\text{N}_3(\text{PF}_6)$  (NDMAP) characterized by similar characteristic parameters as NENB, namely  $J/k_B = 30$  K and  $D/J = 0.25$ . Systematic study of the critical behavior for magnetic fields oriented parallel with the chain axis revealed magnetic ordering at 0.6 K in magnetic field 4 T [32]. Increasing the magnetic field slightly shifted the ordering temperature towards higher values, however, at 1 K, the ordering temperature became field independent. Notably, the shape of the observed sharp  $\lambda$ -like anomaly was altered very little by various magnetic fields. Similar behavior was reported also in Ref. [33], in which a richer phase diagram was found for higher magnetic fields. In NENB an indication of magnetic ordering was observed only at 9 T, such ordering still might be anticipated at lower temperatures due to presumably weaker  $J'$  than existing in NDMAP. Given that thermodynamic properties of NDMAP and NENB are similar, analogous behavior of a  $\lambda$ -like anomaly, although at lower temperatures, may be anticipated in NENB. The robustness of the shape of the peak in specific heat to the alternation of magnetic field leads to its basically constant entropy content. Consequently, in this approximation, not taking into account the contribution of a  $\lambda$ -like anomaly to magnetic entropy leads to systematic, but constant shift of the values of magnetic entropy, however, the isentropes may not necessarily be influenced. Thus, the existence of interchain exchange interaction itself does not seem to be responsible for the onset of normal MCE at low temperatures/magnetic fields.

The existence of single-ion anisotropy in NENB may represent another reason for the deviation of the isentropes

from the predicted behavior. Indeed, change of the energy levels due to single-ion anisotropy obviously leads to change in specific heat and subsequently in magnetocaloric response. Focusing on magnetocaloric behavior at low temperatures the effect of the anisotropy was addressed using a simplified model in which only the ground state and the first excited state was considered. For quantum chains with the Haldane gap, planar anisotropy splits the first excited triplet into a lower lying doublet and singlet located above it. In addition, in-plane anisotropy further splits the doublet into two singlets. This energy level scheme for the excited state was adopted to interpret ESR spectra of NENB [20]. Taking into account the results of ESR analysis, magnetocaloric behavior was studied for the same energy level scheme with  $D/k_B = 7.5$  K and  $E/k_B = 0.5$  K for magnetic fields oriented both parallel and perpendicular to the axis of quantization. The corresponding isentropes are presented in Figs. 5(a) and 5(b). Notably, both sets of isentropes retain features of magnetocaloric behavior found for the isotropic  $S = 1$  HAF chain. More specifically, for magnetic fields smaller than  $B_c$ , the inverse MCE dominates, whereas for  $B > B_c$  change of a regime is found. Unlike MCE in quantum spin chains, pronounced normal MCE is found at higher magnetic fields. However, no sign of a normal MCE is indicated for  $B < B_c$ , thus crystal field anisotropy does not seem to be responsible for magnetocaloric behavior found in NENB at lowest temperatures and magnetic fields.

Finally,  $S = 1/2$  states from the ends of chain segments can be considered. Having acquired an estimation of their concentration and considering the single value of ferromagnetic interaction from the analysis of specific heat in zero magnetic field, their contribution to MCE can be calculated exactly and the evaluated isentropes are presented in Fig. 4. It can be immediately seen that these degrees of freedom are characterized by normal MCE in the parametric region of the interest and their isentropes correspond reasonably with those found for NENB at least for magnetic fields from 2 to 4 T. Their contribution is becoming more pronounced with decreasing temperature in accord with the experimental observation. However, no inflection point is indicated in the calculated isentropes, in contrast with those found for NENB. Two features may be responsible for this discrepancy. First, taking into account randomness in the lengths of the chain segments in NENB and consequently randomness of spatial arrangement of  $S = 1/2$  degrees of freedom a distribution of the magnitudes of exchange coupling may be anticipated. Second, the existence of various types of terminating units in the segments and/or their different spatial arrangement may lead to the onset of also antiferromagnetic coupling. Clearly, spin glass behavior reported for NENB supports the scenario based on the distribution of the magnitudes of exchange coupling and potential coexistence of anti- and ferromagnetic interactions among  $S = 1/2$  degrees of freedom. Obviously, considering distributions of both anti- and ferromagnetic interactions together with unknown concentration of  $S = 1/2$  degrees of freedom represents an overparametrized task for fitting specific heat data in zero magnetic field. Yet, using even the simplified model captures the main features of the observed behavior and suggests that  $S = 1/2$  degrees of freedom may govern the observed magnetocaloric behavior in NENB at low temperatures and low magnetic fields.

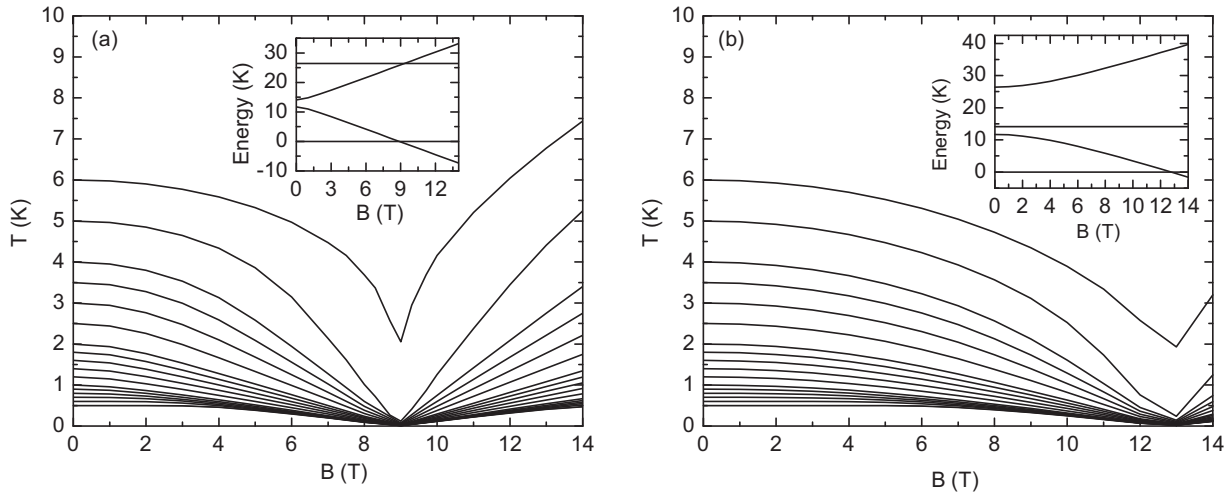


FIG. 5. Adiabatic demagnetization curves calculated for the simplified energy level scheme for a Haldane system, considering only a singlet ground state and the first excited triplet with  $D/k = 7.5$  K and  $E/k = 0.7$  K for magnetic fields oriented parallel (a) and perpendicular (b) to the axis of quantization. Magnetic field dependences of the energy levels are presented in the insets.

## V. CONCLUSIONS

In summary, MCE of spin-1 chain material NENB was investigated at low temperatures ( $T < 0.5 \Delta/k_B$ ) in magnetic fields up to  $0.11 B_{\text{sat}}$ . The study confirmed theoretically predicted behavior for a quantum spin chain with the Haldane gap in magnetic fields lower than the saturation field. More specifically, two distinct regimes were clearly identified, for  $B < B_c$  inverse MCE was found, which is becoming more pronounced with decreasing temperature. Magnetic fields higher than  $B_c$  induce a different regime in which the excitation spectrum remains gapless with a large degeneracy of modes. Consequently, only a weak MCE is observed in accord with the theoretical prediction. A theoretical suggestion about practical applicability of the inverse MCE might become limited in a real material due to the segmentation of chains and subsequent normal magnetocaloric response of the end chain  $S = 1/2$  degrees of freedom.

These studies may be extended towards the saturation magnetic field, however, for NENB, such a high magnetic field ( $\approx 125$  T) is not commonly accessible. In this context NDMAP might be more appropriate due to a lower value of the exchange coupling and also the absence of staggered  $g$  tensors due to mutual tilting of local anisotropy axes on adjacent Ni sites.

## ACKNOWLEDGMENTS

We would like to thank Ch. Landee for providing us the single crystal of NENB. The work was supported by projects APVV-14-0073 and ITMS 26220120047. The thermodynamic studies were performed in MLTL (see <http://mltl.eu/>), which is supported within the program of Czech Research Infrastructures (Project No. LM2011025).

- 
- [1] F. Pobell, *Matter and Methods at Low Temperatures* (Springer, Berlin, 1992).
  - [2] O. V. Lounasmaa, *Experimental Principles and Methods Below 1 K* (Academic, London, 1974), and references therein.
  - [3] N. Kurti, M. P. Enrico, S. N. Fisher, A. M. Guenault, and I. E. Miller, *Cryogenics* **1**, 2 (1960).
  - [4] G. R. Pickett, K. Torizuka, R. P. Turner, and M. G. Ward, *Physica B* **194**, 47 (1994).
  - [5] O. Tegus, E. J. Brück, K. H. Buschow, and F. R. de Boer, *Nature (London)* **415**, 150 (2002).
  - [6] M. E. Zhitomirsky, *Phys. Rev. B* **67**, 104421 (2003).
  - [7] S. S. Sosin, L. A. Prozorova, A. I. Smirnov, A. I. Golov, I. B. Berkutov, O. A. Petrenko, G. Balakrishnan, and M. E. Zhitomirsky, *Phys. Rev. B* **71**, 094413 (2005).
  - [8] A. Honecker and S. Wessel, *Condens. Matter Phys.* **12**, 399 (2009).
  - [9] Ch. Trippé, A. Honecker, A. Klümper, and V. Ohanian, *Phys. Rev. B* **81**, 054402 (2010).
  - [10] M. E. Zhitomirsky and A. Honecker, *J. Stat. Mech.: Theor. Exp.* (2004) P07012.
  - [11] L. Čanová, J. Strečka, and T. Lučivjanský, *Condens. Matter Phys.* **12**, 353 (2009).
  - [12] M. Topilko, T. Krokhumalskii, O. Derzhko, and V. Ohanian, *Eur. Phys. J. B* **85**, 278 (2012).
  - [13] B. Schmidt, P. Thalmeier, and N. Shannon, *Phys. Rev. B* **76**, 125113 (2007).
  - [14] D. Straßel, P. Kopietz, and S. Eggert, *Phys. Rev. B* **91**, 134406 (2015).
  - [15] O. Castillo, A. Luge, J. Sertucha, P. Roman, and F. Lloret, *Inorg. Chem.* **39**, 6142 (2000).
  - [16] B. Wolf, Y. Tsui, D. Jaiswal-Nagar, U. Tutsch, A. Honecker, K. Remović-Langer, G. Hofmann, A. Prokofiev, W. Assmus, G. Donath, and M. Lang, *PNAS* **108**, 6862 (2011).
  - [17] R. Tarasenko, E. Čižmár, A. Orendáčová, J. Kuchár, J. Černák, J. Prokleška, V. Sechovský and M. Orendáč, *Solid State Sci.* **28**, 14 (2014).

- [18] B. Willenberg, H. Ryll, K. Kiefer, D. A. Tennant, F. Groitl, K. Rolfs, P. Manuel, D. Khalyavin, K. C. Rule, A. U. B. Wolter, and S. Süllow, *Phys. Rev. B* **91**, 060407(R) (2015).
- [19] A. S. Boyarchenkov, I. G. Bostrem, and A. S. Ovchinnikov, *Phys. Rev. B* **76**, 224410 (2007).
- [20] E. Čížmár, M. Ozerov, O. Ignatchik, T. P. Papageorgiou, J. Wosnitza, S. A. Zvyagin, J. Krzystek, Z. Zhou, C. P. Landee, and B. R. Landry, *New J. Phys.* **10**, 033008 (2008).
- [21] V. C. Long, Y.-H. Chou, I. A. Cross, A. C. Kozen, J. R. Montague, E. C. Schundler, X. Wei, S. A. McGill, B. R. Landry, K. R. Maxcy-Pearson, M. M. Turnbull, and C. P. Landee, *Phys. Rev. B* **76**, 024439 (2007).
- [22] Cambridge Crystallographic Data Center, deposition number 638437.
- [23] A. Meyer, A. Gleizes, J. Girerd, M. Verdaguer, and O. Kahn, *Inorg. Chem.* **21**, 1729 (1982).
- [24] H. W. J. Blöte, *Physica B+C* **79**, 427 (1975).
- [25] M. Ito, M. Mito, H. Deguchi, and K. Takeda, *J. Phys. Soc. Jpn.* **63**, 1123 (1994).
- [26] I. Affleck, T. Kennedy, E. H. Lieb, and H. Tasaki, *Phys. Rev. Lett.* **59**, 799 (1987).
- [27] M. Hagiwara, K. Katsumata, I. Affleck, B. I. Halperin, and J. P. Renard, *Phys. Rev. Lett.* **65**, 3181 (1990); T. C. Kobayashi, H. Honda, A. Koda, and K. Amaya, *J. Phys. Soc. Jpn.* **64**, 2609 (1995).
- [28] M. Hagiwara, N. Narita, and I. Yamada, *Phys. Rev. B* **55**, 5615 (1997).
- [29] L. Zhu, M. Garst, A. Rosch, and Q. Si, *Phys. Rev. Lett.* **91**, 066404 (2003); M. Garst and A. Rosch, *Phys. Rev. B* **72**, 205129 (2005).
- [30] T. Sakai and M. Takahashi, *Phys. Rev. B* **42**, 4537 (1990).
- [31] T. Nikuni, M. Oshikawa, A. Oosawa, and H. Tanaka, *Phys. Rev. Lett.* **84**, 5868 (2000).
- [32] Z. Honda, H. Asakawa, and K. Katsumata, *Phys. Rev. Lett.* **81**, 2566 (1998).
- [33] H. Tsujii, Z. Honda, B. Andraka, K. Katsumata, and Y. Takano, *Phys. Rev. B* **71**, 014426 (2005).